Hindawi Publishing Corporation
Journal of Nanoparticles
Volume 2014, Article ID 285954, 6 pages
http://dx.doi.org/10.1155/2014/285954

Research Article

Synthesis of Platinum Nanoparticles from K_2PtCl_4 Solution Using Bacterial Cellulose Matrix

H. F. Aritonang,[1,2] D. Onggo,[1] C. Ciptati,[3] and C. L. Radiman[1]

[1]*Inorganic and Physical Chemistry Division, Faculty of Mathematics and Natural Sciences, Institut Teknologi Bandung, Jalan Ganesha 10, Bandung 40132, Indonesia*
[2]*Physical Chemistry Division, Faculty of Mathematics and Natural Sciences, Universitas Sam Ratulangi, Jalan Kampus UNSRAT Kleak, Manado 95115, Indonesia*
[3]*Organic Chemistry Division, Faculty of Mathematics and Natural Sciences, Institut Teknologi Bandung, Jalan Ganesha 10, Bandung 40132, Indonesia*

Correspondence should be addressed to C. L. Radiman; cynthia@mail.chem.itb.ac.id

Received 9 May 2014; Revised 12 November 2014; Accepted 16 November 2014; Published 14 December 2014

Academic Editor: Vijaya Rangari

Platinum (Pt) nanoparticles have been synthesized from a precursor solution of potassium tetrachloroplatinate (K_2PtCl_4) using a matrix of bacterial cellulose (BC). The formation of Pt nanoparticles occurs at the surface and the inside of the BC membrane by reducing the precursor solution with a hydrogen gas reductant. The Pt nanoparticles obtained from the variations of precursor concentration, between 3 mM and 30 mM, and the formation of Pt nanoparticles have been studied using X-ray diffraction (XRD), scanning electron microscopy-energy dispersive X-ray spectroscopy (SEM-EDS), and thermogravimetry analysis (TGA). Based on X-ray diffraction patterns, Pt particles have sizes between 6.3 nm and 9.3 nm, and the Pt particle size increases with an increase in precursor concentration. The morphology of the Pt nanoparticles was observed by SEM-EDS and the content of Pt particles inside the membrane is higher than that on the surface of BC membranes. This analysis corresponds to the TGA analysis, but the TGA analysis is more representative in how it describes the content of Pt particles in the BC membrane.

1. Introduction

Platinum (Pt) has attracted much attention because Pt is the best catalyst to use for a variety of specific purposes. As a noble metal, Pt has the best catalytic activity among all pure metals, especially in fuel cells [1]. Many factors affect the electrocatalytic activity of Pt particles, such as the size, distribution, and synthesis method [2, 3]. The catalytic activity of Pt is better when nanosized Pt particles are produced. A nanosized Pt catalyst that is distributed properly will result in high electrocatalytic activity [1, 4, 5]. To synthesize nanosized Pt particles, several methods have been applied, such as colloidal systems [6], reduction [7], using bacterial cellulose (BC) as a hydrophilic matrix [8], microemulsion [9], sol-gel [10], sonochemical method [11], and electrodeposition [12]. However, no one method is superior to the other methods because it depends on the final application of the catalyst used.

Among these methods, the synthesis of Pt nanoparticles using the reduction method is a very simple method. This method is done by reducing the precursor solution with a reducing agent. The precursors that are most often used as a source of Pt particles are H_2PtCl_6 and the reducing agents, that are also commonly used, are formaldehyde [13], Lithium triethylborohydride [14], sodium borohydride [15], and ethylene glycol [16]. Yang et al. [17] have synthesized Pt nanoparticles from Pt (IV) solution, namely, H_2PtCl_6, into BC matrix using sodium borohydride and a formaldehyde reductant. They reported that the Pt particle sizes of 3-4 nm are generated and applied as catalysts for fuel cells. This research has inspired us to synthesize Pt nanoparticles using precursor Pt (II) instead of Pt (IV). BC has been known as a matrix that synthesizes some of the nanometals, such as palladium and silver. BC has the ability of a matrix because the fiber structure of BC has a cavity that is used as a minireactor for the synthesis of nanoparticles [8].

The present study uses the precursor Pt (II) of K_2PtCl_4 as a source of Pt particles and hydrogen gas as the reducing agent. By using a precursor source and reducing agent that differs from previous research, this research is expected to provide new information on the synthesis development of Pt nanoparticles, particularly for use in fuel cells.

2. Materials and Methods

2.1. Materials. Potassium tetrachloroplatinate (II) (K_2PtCl_4) was obtained from Sigma-Aldrich (99,9%), while ammonium sulfate, glacial acetic acid, hydrochloric acid, sodium hydroxide, and ethanol were obtained from Merck. Hydrogen gas (ultra-highly pure) was obtained from a local supplier. Coconut water, sucrose (food-grade white sugar), and *Acetobacter xylinum* were obtained from a local traditional market. All chemicals were used without further purification.

2.2. Preparation of BC. Preparation of BC was carried out as described previously by Radiman and Yuliani [18]. To obtain dry BC membranes, the BC was first cut to a size of 4 cm × 4 cm, then pressed to remove water, and finally air dried at room temperature for 6 days. Dried BC membrane was used for analysis by SEM-EDS.

2.3. Synthesis of Pt Nanoparticles Impregnated into BC. The pressed BC hydrogels were soaked in aqueous K_2PtCl_4 solutions, with different concentrations (3 mM, 5 mM, 10 mM, 20 mM, and 30 mM), for 2 hrs and sonicated at room temperature for another 2 hrs. The BC gel was removed, rinsed with deionized water, and soaked again in deionized water. The Pt (II) was then reduced with hydrogen gas at an applied constant pressure of 0.5 psi and a stirring speed of 500 rpm at room temperature for 1 hr. Pt-BC gel was removed from the solution and dried, as in the above procedure, and produced a dry composite membrane that is denoted by Pt-BCcm. The thickness of the resulting Pt-BCcm membrane was 0.5–0.7 mm.

2.4. X-Ray Analysis. X-ray diffraction (XRD) patterns were recorded on an X-ray diffractometer (PW1710, Philips), using Cu Kα radiation ($\lambda = 1,54060$ Å) at 40 kV and 30 mA. The diffraction angle ranged from 5 to 90°. The crystallite size of the Pt nanoparticles was calculated based on X-ray diffraction measurements. The crystallite size was calculated from the full width at half maximum (FWHM) of peak using the Scherrer formula [19]:

$$L = \frac{K\lambda}{\beta \cos\theta}, \quad (1)$$

where L is the average crystallite size of the Pt particles, K is a constant of 0.9, λ is the X-ray wavelength, β is the FWHM in radians, and θ is the diffraction angle.

2.5. Scanning Electron Microscopy (SEM) and Energy Dispersive X-Ray Spectroscopy (EDS) Analysis. SEM was used to observe the BC membrane and the distribution of Pt nanoparticles in Pt-BCcm membrane. The BC membrane was coated with a thin layer of evaporated gold, whereas the Pt-BCcm membrane was scanned without being coated. For cross-sectional morphology and line analysis, the Pt-BCcm membrane was cut using liquid nitrogen. The images were taken using a JEOL, JSM-6510 LA scanning electron microscopy (Japan) with an acceleration voltage of 15 kV. Energy dispersive X-ray spectroscopy (EDS) was used for the elemental analysis of the surface and the inner part of the Pt-BCcm membranes.

2.6. Thermogravimetric Analysis (TGA). Thermal properties of the Pt-BCcm membrane were investigated by thermogravimetric analysis (TG, NETZSCH STA 449F1 instruments), in conjunction with a thermal analysis controller. The samples were kept in an alumina crucible and heated in a furnace, flushed with nitrogen gas at the rate of 40 mL/min, from 30°C to 800°C, at a heating rate of 10°C/min. The percentage of weight loss was plotted against temperature for all the samples. The content of Pt (in mg/cm^2) in Pt-BCcm membranes was obtained from the difference between the residual mass of the Pt-BCcm membrane and the BC membrane as a control.

3. Results and Discussion

3.1. XRD Analysis. Pt nanoparticles have been successfully synthesized from aqueous K_2PtCl_4 solution inside the BC membrane using hydrogen gas as a reducing agent. The evidence of Pt nanoparticles in Pt-BCcm membrane is shown by the X-ray diffraction spectrum, in Figure 1.

Basically, all of Pt-BCcm membranes containing Pt (0) (from all precursor concentrations) gave diffraction patterns that were similar; the differences lie in the concentration of the Pt precursor. When the precursor concentration was 3 mM, Pt crystal diffraction peaks that appeared had only two peaks, at area of $2\theta = 39.5°$ and 46.1°. By the time the concentration was increased to 5 mM, Pt crystal diffraction displayed four peaks; these appear in addition to the two peaks at the concentration of 3 mM, coupled with a peak at $2\theta = 67.9°$ and 81.2°. Pt particle diffraction pattern peaks are in accordance with their respective crystal planes (111), (200), (220), and (311), as shown in the ICSD database of Pt number 76951. In addition, it appears that the peak intensity of the Pt crystal becomes higher when the concentration of the Pt precursor is greater and so is the impact on the increasing content of Pt particles in the Pt-BCcm membrane. Based on the Pt diffraction pattern of the Pt database from ICSD number 76951, it is evident that the Pt precursor solution has reduced yields of Pt particles.

X-ray diffraction patterns also indicate that, besides the characteristic Pt peaks, characteristic peaks of BC in the area $2\theta = 14.2°$, 16.6°, and 22.4° also appear. A BC peak appeared in each Pt-BCcm membrane. BC diffraction patterns were similar to those done by previous researchers [20, 21]. However, increasing the concentration of the Pt precursor decreases the peak intensity of the BC peak areas, especially the area at $2\theta = 14.2°$ and 16.6°.

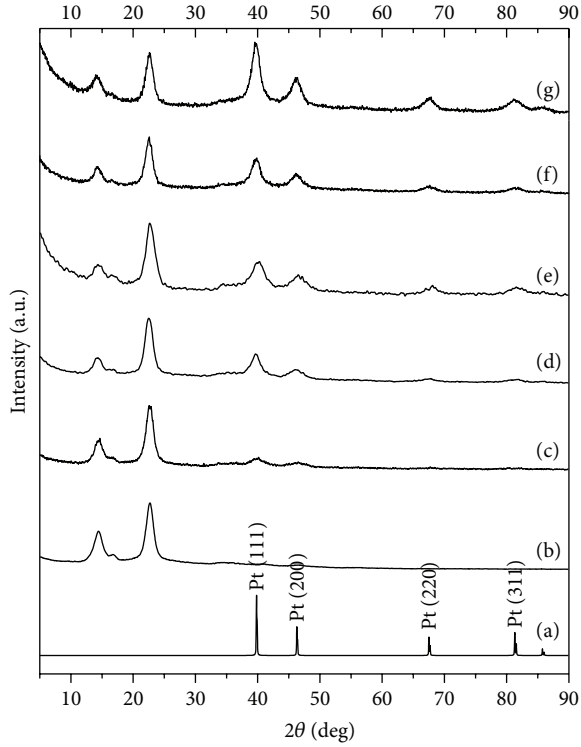

Figure 1: X-ray diffraction patterns of (a) Pt (taken from database: ICSD number 76951), (b) BC membrane, and (c–g) Pt-BCcm membrane (obtained from K_2PtCl_4 solution at 3 mM, 5 mM, 10 mM, 20 mM, and 30 mM, resp.).

Table 1: The average crystallite size of Pt nanoparticles.

Precursor concentration [mM]	Average Pt crystallite size [nm]
3	6.3
5	6.8
10	8.3
20	8.9
30	9.3

The Pt(111) peak is used as a reference in calculating the size of the average Pt crystal because its intensity is the highest among the other peaks. Table 1 shows the size of the average Pt crystals which were calculated from FWHM (111) peak using the Scherrer formula.

3.2. SEM Observation. The formation of Pt particles on the BC membrane is visually observed through a color change in the BC membrane. The BC membrane was originally transparent white, but it changed to black when Pt was inserted in the BC membrane. The change of membrane to black indicates that Pt (II) ions have been successfully reduced and deposited on the fibers of BC. However, there were no obvious color differences among the composites obtained by different concentrations of the precursor.

Observation on the surface morphology of the Pt-BCcm membrane showed that white granules were embedded in the BC membrane and that the grains are Pt particles. White grain indicates that Pt particles have been formed and deposited in the cavity of the BC matrix. Deposition of Pt particles formed agglomerations or clusters at a certain level. At low precursor concentration, only a few Pt particles were visible, but at higher precursor concentrations, the amount of Pt particles was more and had a larger size, indicating that formed agglomerations are large. SEM images of the surface morphology on the Pt-BCcm membrane can be seen in Figure 2.

Based on SEM images, the Pt particle size seems large because of the occurrence of agglomeration. Meanwhile, an analysis by using X-ray diffraction patterns shows that the size of the Pt crystals is nanoscale for all precursor concentrations. This difference is due to the X-ray diffraction pattern analysis that describes the size of the Pt crystals contained in Pt particles, because Pt particles are formed from collections of Pt crystals. Therefore, both analyses look different in analyzing the Pt particle size.

The formation of Pt particles appears not only on the BC membrane surface but also on the inside of the BC fiber. Pt particles are formed on the inside of the BC fibers; this is known from the cross-sectional SEM images of the Pt-BCcm membrane. The presence of Pt particles on the inside of the BC fibers also shows that the precursor solution entered into the inner BC fibers and interacted with BC cellulose. Therefore, when reduction occurs, Pt particles are trapped on the inside (between the fibers) of BC, as shown in Figure 3.

3.3. Analysis of the Content of Pt Particles. The content of Pt particles in the Pt-BCcm membrane, both on the surface and on the inside of the membrane, has been analyzed by EDX. The content of Pt particles on the inside of the membrane appears to be higher than that on the membrane surface of Pt-BCcm. At concentration of 30 mM, the content of Pt particles remained higher on the inside of the membrane compared to the membrane surface, 3.24 mg/cm^2 and 3.37 mg/cm^2, respectively. Relations between precursor concentration and the content of Pt particles, for both the inside of Pt-BCcm and its membrane surface, are shown in Figure 4.

The high content of Pt particles on the inside of the Pt-BCcm membrane can be explained through the formation mechanism of Pt particles in the BC matrix. The formation mechanism applies to the surface and inner membranes. At the initial stage, the precursor dissociates in water, according to the following reaction:

$$K_2PtCl_{4(aq)} \longrightarrow [PtCl_4]_{(aq)}^{2-} + 2K_{(aq)}^{+} \quad (2)$$

Then, $[PtCl_4]^{2-}$ ions undergo solvolysis reaction [22, 23]:

$$[PtCl_4]_{(aq)}^{2-} + H_2O_{(l)} \longrightarrow PtCl_3(H_2O)_{(aq)}^{-} + Cl_{(aq)}^{-} \quad (3)$$

$$PtCl_3(H_2O)_{(aq)}^{-} + H_2O_{(l)} \longrightarrow PtCl_2(H_2O)_{2(aq)} + Cl_{(aq)}^{-} \quad (4)$$

The existence of solvolysis products $PtCl_2(H_2O)_2$ that are formed in K_2PtCl_4 solution means that the interaction with

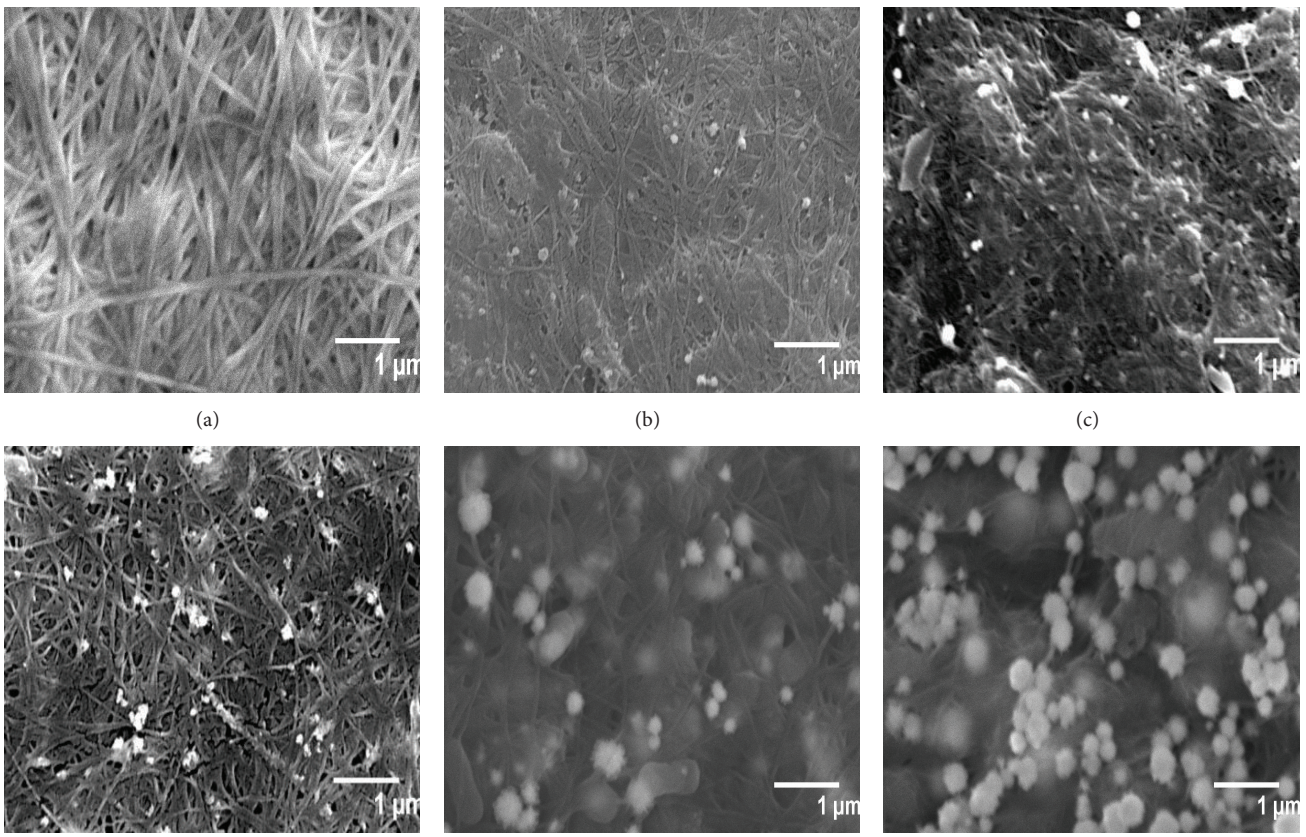

Figure 2: SEM images of (a) dried BC and (b)–(f) Pt-BCcm membrane (obtained from K_2PtCl_4 solution at 3 mM, 5 Mm, 10 mM, 20 mM, and 30 mM, resp.).

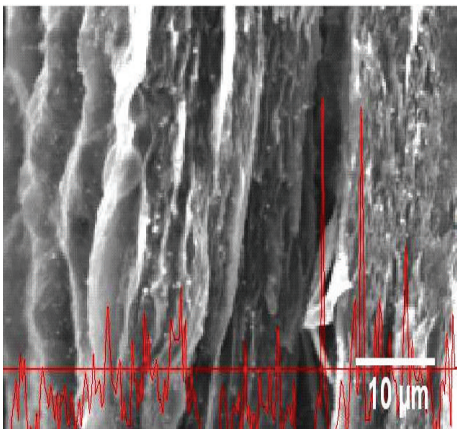

Figure 3: SEM images of Pt-BCcm cross section prepared from 10 mM K_2PtCl_4.

BC cellulose can occur through hydrogen bonding. Hydrogen bonding is between the O atoms of BC cellulose, with H atoms of $PtCl_2(H_2O)_2$ and the O atoms of $PtCl_2(H_2O)_2$, and also with H atoms from BC cellulose. Hydrogen bonding occurs on the surface and the inner of the BC membrane, as shown in Scheme 1.

When the reduction process takes place, the Pt particles are formed on the surface and the inner of BC membrane:

$$PtCl_2\,(H_2O)_{2(aq)} + H_{2(g)} \longrightarrow Pt_{(s)} + 2Cl_{(aq)}^{-} + 2H_2O_{(l)} + 2H_{(aq)}^{+} \quad (5)$$

The Pt particles that were formed on the membrane surface were easily separated during the reduction process, whereas it was tough for the inside of membrane because of Pt particles in between the fibers of BC. This results in the Pt particles content on the inside of the membrane being higher than that in the BC membrane surface. This analysis indicates that the BC is able to stabilize the Pt particles in the three-dimensional nanostructure of BC. Thus, the overall reaction of the formation of Pt particles is as follows:

$$K_2\,[PtCl_4]_{(aq)} + H_{2(g)} \longrightarrow Pt_{(s)} + 2H_{(aq)}^{+} + 2K_{(aq)}^{+} + 4Cl_{(aq)}^{-} \quad (6)$$

However, the content of Pt particles in the Pt-BCcm membrane is different for the EDX analysis, when analyzed using the thermal analysis (TGA). Burning the Pt-BCcm membrane in the furnace to a temperature of 800°C results in residue that is assumed to be the total amount of Pt per cm^2 of

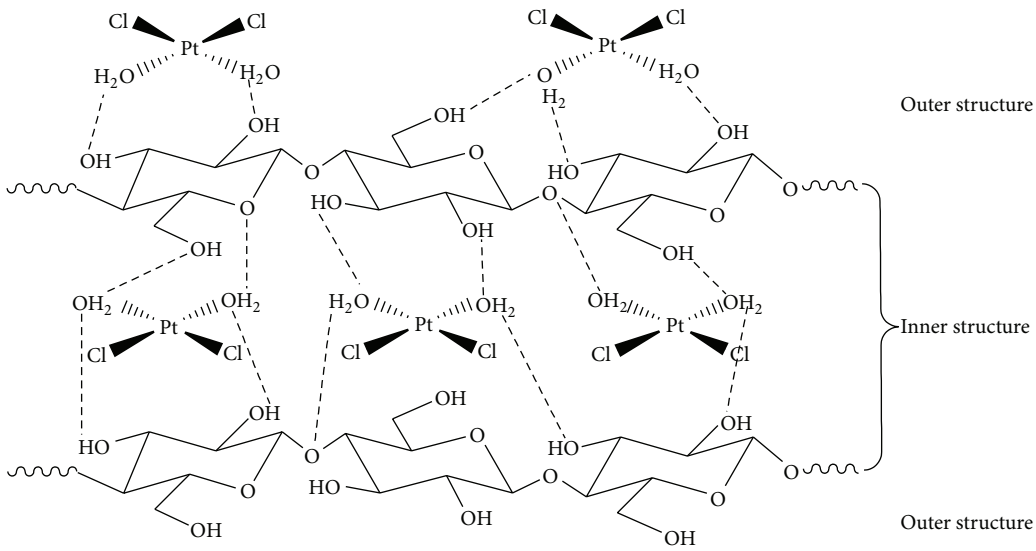

Scheme 1: Schematic illustration of the hydrogen bonding between BC and $PtCl_2(H_2O)_2$ at the BC structure (- - - - - hydrogen bonding).

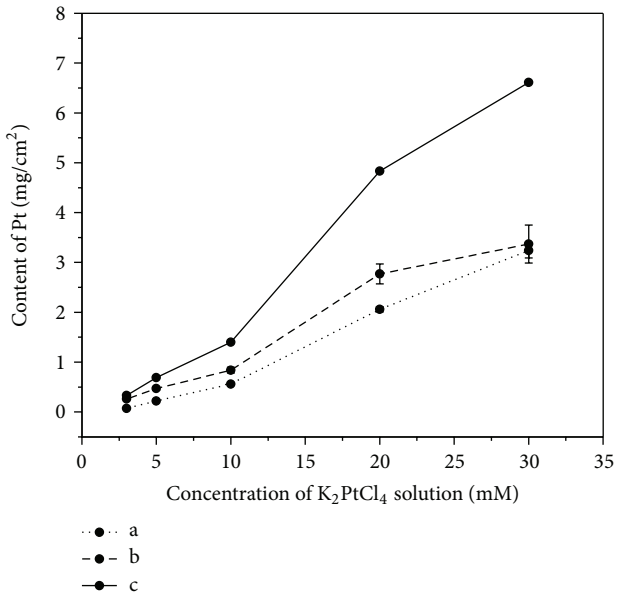

Figure 4: Effect of K_2PtCl_4 concentration on Pt content (a) on the membrane surface, (b) inside of the membrane, and (c) total on the surface and inside of the membrane.

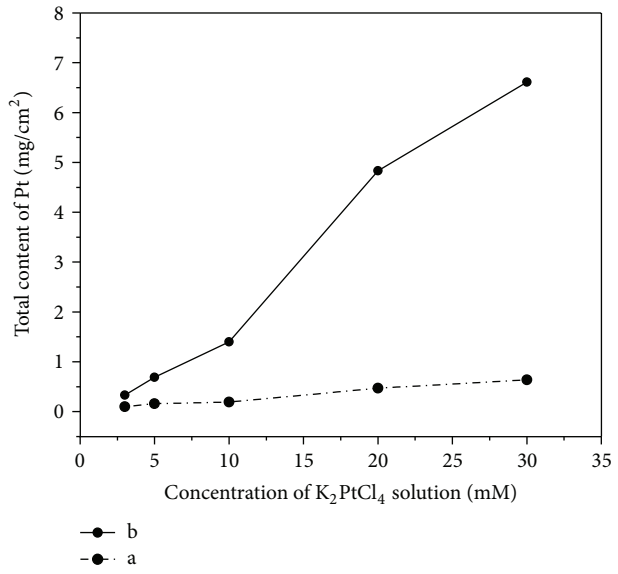

Figure 5: Comparison of the Pt content on the Pt-BCcm membrane based on (a) TGA data and (b) EDS data.

the Pt-BCcm membrane. When the precursor concentration is increased from 3 mM to 10 mM, the content of Pt particles is significantly increased. Furthermore, when the precursor concentration is increased above 10 mM, the increase in the content of Pt particles in the Pt-BCcm membrane is significant. At a precursor concentration of 30 mM, Pt particle content reached 0.64 mg/cm^2 and 6.61 mg/cm^2, respectively, based on the TGA and EDX analysis. Comparisons of Pt particle content in the Pt-BCcm membrane, based on two analyses, are shown in Figure 5.

This information indicates that the analyses on the Pt particle content of the Pt Pt-BCcm membrane, by using these two methods, are very different, so that it can be said that the Pt particles on the BC membrane are less evenly distributed. However, the TGA analysis is more representative in analyzing the content of Pt particles in the Pt-BCcm membrane compared to the EDX analysis.

4. Conclusions

Pt nanoparticles have been synthesized from the K_2PtCl_4 solution using H_2 as a reducing agent. The presence of Pt particles has been demonstrated through the analysis

of X-ray diffraction and BC membrane discoloration, from transparent white to black. The presence of Pt nanoparticles is found not only on the membrane surface, but also on the inside of the Pt-BCcm membrane. Based on SEM images, the Pt particle size increases with an increasing precursor concentration, from nanometers to micrometer size. However, based on the XRD analysis that uses Scherrer equation, the Pt crystal size was obtained between 6.3 nm and 9.3 nm, and the size increased with an increasing precursor concentration. The content of Pt particles on the inside of the membrane is higher than that on the surface of the membrane.

Conflict of Interests

The authors declare that there is no conflict of interests regarding the publication of this paper.

Acknowledgment

This work was financially supported by the *Lembaga Penelitian dan Pengabdian Masyarakat*-ITB under the *Riset & Inovasi KK-ITB 2013* program, contract no. 267/I.1.C01/PL/2013.

References

[1] D.-H. Lim, W.-D. Lee, and H.-I. Lee, "Highly dispersed and nano-sized Pt-based electrocatalysts for low-temperature fuel cells," *Catalysis Surveys from Asia*, vol. 12, no. 4, pp. 310–325, 2008.

[2] Y. Takasu, N. Ohashi, X.-G. Zhang et al., "Size effects of platinum particles on the electroreduction of oxygen," *Electrochimica Acta*, vol. 41, no. 16, pp. 2595–2600, 1996.

[3] K. Bergamaski, A. L. N. Pinheiro, E. Teixeira-Neto, and F. C. Nart, "Nanoparticle size effects on methanol electrochemical oxidation on carbon supported platinum catalysts," *The Journal of Physical Chemistry B*, vol. 110, no. 39, pp. 19271–19279, 2006.

[4] Z. He, J. Chen, D. Liu, H. Tang, W. Deng, and Y. Kuang, "Deposition and electrocatalytic properties of platinum nanoparticals on carbon nanotubes for methanol electrooxidation," *Materials Chemistry and Physics*, vol. 85, no. 2-3, pp. 396–401, 2004.

[5] C. V. Rao and B. Viswanathan, "Monodispersed platinum nanoparticle supported carbon electrodes for hydrogen oxidation and oxygen reduction in proton exchange membrane fuel cells," *Journal of Physical Chemistry C*, vol. 114, no. 18, pp. 8661–8667, 2010.

[6] M. P. Pileni, "Nanosized particles made in colloidal assemblies," *Langmuir*, vol. 13, no. 13, pp. 3266–3276, 1997.

[7] S.-H. Wu and D.-H. Chen, "Synthesis and characterization of nickel nanoparticles by hydrazine reduction in ethylene glycol," *Journal of Colloid and Interface Science*, vol. 259, no. 2, pp. 282–286, 2003.

[8] B. R. Evans, H. M. O'Neill, V. P. Malyvanh, I. Lee, and J. Woodward, "Palladium-bacterial cellulose membranes for fuel cells," *Biosensors and Bioelectronics*, vol. 18, no. 7, pp. 917–923, 2003.

[9] M. Sanchez-Dominguez, M. Boutonnet, and C. Solans, "A novel approach to metal and metal oxide nanoparticle synthesis: the oil-in-water microemulsion reaction method," *Journal of Nanoparticle Research*, vol. 11, no. 7, pp. 1823–1829, 2009.

[10] H. B. Suffredini, G. R. Salazar-Banda, and L. A. Avaca, "Carbon supported electrocatalysts prepared by the sol-gel method and their utilization for the oxidation of methanol in acid media," *Journal of Sol-Gel Science and Technology*, vol. 49, no. 2, pp. 131–136, 2009.

[11] C. A. Angelucci, M. D'Villa Silva, and F. C. Nart, "Preparation of platinum-ruthenium alloys supported on carbon by a sonochemical method," *Electrochimica Acta*, vol. 52, no. 25, pp. 7293–7299, 2007.

[12] J. M. Sieben, M. M. E. Duarte, and C. E. Mayer, "Supported Pt and Pt-Ru catalysts prepared by potentiostatic electrodeposition for methanol electrooxidation," *Journal of Applied Electrochemistry*, vol. 38, no. 4, pp. 483–490, 2008.

[13] Z. Zhou, S. Wang, W. Zhou et al., "Preparation of highly active Pt/C cathode electrocatalysts for DMFCs by an improved aqueous impregnation method," *Physical Chemistry Chemical Physics*, vol. 5, no. 24, pp. 5485–5488, 2003.

[14] F. Şen and G. Gökağaç, "Different sized platinum nanoparticles supported on carbon: an XPS study on these methanol oxidation catalysts," *The Journal of Physical Chemistry C*, vol. 111, no. 15, pp. 5715–5720, 2007.

[15] T. Maiyalagan, T. O. Alaje, and K. Scott, "Highly stable Pt-Ru nanoparticles supported on three-dimensional cubic ordered mesoporous carbon (Pt-Ru/CMK-8) as promising electrocatalysts for methanol oxidation," *The Journal of Physical Chemistry C*, vol. 116, no. 3, pp. 2630–2638, 2012.

[16] Y. Wu, S. Liao, K. Wang, M. Chen, and V. Birss, "High pressure organic colloid method for the preparation of high performance carbon nanotube-supported Pt and PtRu catalysts for fuel cell applications," *Science in China Series E: Technological Sciences*, vol. 53, no. 1, pp. 264–271, 2010.

[17] J. Yang, D. Sun, J. Li et al., "*In situ* deposition of platinum nanoparticles on bacterial cellulose membranes and evaluation of PEM fuel cell performance," *Electrochimica Acta*, vol. 54, no. 26, pp. 6300–6305, 2009.

[18] C. Radiman and G. Yuliani, "Coconut water as a potential resource for cellulose acetate membrane preparation," *Polymer International*, vol. 57, no. 3, pp. 502–508, 2008.

[19] A. Monshi, M. R. Foroughi, and M. R. Monshi, "Modified scherrer equation to estimate more accurately nano-crystallite size using XRD," *World Journal of Nano Science and Engineering*, vol. 2, pp. 154–160, 2012.

[20] K.-C. Cheng, J. M. Catchmark, and A. Demirci, "Effect of different additives on bacterial cellulose production by *Acetobacter xylinum* and analysis of material property," *Cellulose*, vol. 16, no. 6, pp. 1033–1045, 2009.

[21] A. Retegi, N. Gabilondo, C. Peña et al., "Bacterial cellulose films with controlled microstructure-mechanical property relationships," *Cellulose*, vol. 17, no. 3, pp. 661–669, 2010.

[22] C. I. Sanders and D. S. Martin Jr., "Acid hydrolysis of $[PtCl_4]$- and $[PtCl_3(H_2O)]^{-1}$," *Journal of the American Chemical Society*, vol. 83, no. 4, pp. 807–810, 1961.

[23] F. A. Cotton, G. Wilkinson, C. A. Murillo, and M. Bochmann, *Advanced Inorganic Chemistry*, John Wiley & Sons, New York, NY, USA, 6th edition, 1999.